

This is a pre-print of an article published in *Nonlinear Dynamics*. The final authenticated version is available online at: <https://doi.org/10.1007/s11071-015-2436-z>

Strange attractors generated by a fractional order switching system and its topological horseshoe

E. Zambrano-Serrano · E. Campos-Cantón · J. M. Muñoz-Pacheco

Received: date / Accepted: date

Abstract Chaos generation in a new fractional order unstable dissipative system with only two equilibrium points is reported. Based on the integer version of a unstable dissipative system (UDS) and using the same system's parameters as interger-order, fractional chaos behavior is observed with an order less than three, i.e., 2.85. The fractional order can be decreased as low as 2.4 varying the equilibrium points of the fractional UDS in accordance with a switching law that fulfills the asymptotic stability theorem for fractional systems. The largest Lyapunov exponents are computed from the numerical time series in order to prove the chaos regime. Besides, the presence of fractional chaos is also verified obtaining the topological horseshoe in both cases. That topological proof guarantees the chaos generation in the proposed fractional order switching system avoiding the possible numerical bias of Lyapunov exponents.

Keywords Fractional order · Chaotic system · Strange attractor · Topological horseshoe · UDS

1 Introduction

During the last years fractional calculus starts to attract attention of physicists and engineers due to the fractional order models give more accuracy results than

the corresponding integer-order models [1]-[9]. There are two main features for that claim; the fractional order parameter improves the system performance by increasing one degree of freedom, and the other one is related to fractional derivatives provides a valuable tool for the description of memory and hereditary properties in various processes [4]. Therefore, the fractional derivatives have been used to describe elegantly interdisciplinary applications; for instance, in control theory a fractional order controller has a unique isodamping property that improves robustness via reducing the sensitivity of the system stability margins with respect to the system uncertainties [5]; in viscoelastic materials, the fractional order damping element provides a better model due its modeled as a force proportional to the fractional order derivative to displacement [7]; also in dielectric polarization [8], and so on [9], [10].

One of the main objectives in the literature about fractional calculus is to find chaos behavior in fractional order systems. Usually chaotic attractors cannot be observed in nonlinear systems whose order is less than three, so it is highly interesting to analyze the routes to get fractional chaos. Recently there has been a trend to transform integer-order chaotic systems in fractional versions because of the integer-order versions preserve chaotic dynamics when their models become fractional [10],[11]; such as, the fractional Lorenz system [12], the fractional Chen system [13], the fractional Chua's circuit [14], the fractional Rössler system [15], the fractional jerk system [16], the fractional Lü system [17], and many others [18]. Compared to integer-order, the fractional chaotic systems have the following advantages; the fractional derivatives have complex geometrical interpretation because of their non-local character and high nonlinearity; the power spectrum of fractional order chaotic systems fluctuates com-

E. Zambrano-Serrano · E. Campos-Cantón
Department of Applied Mathematics, Instituto Potósino de Investigación Científica y Tecnológica, San Luis Potosí, SLP., MEXICO, C.P. 78216.
E-mail: ernesto.zambrano@ipicyt.edu.mx

J. M. Muñoz-Pacheco
Faculty of Electronics Sciences, Benemérita
Universidad Autónoma de Puebla, Puebla, Pue., MEXICO,
C.P. 72570.

plexly increasing the chaoticity in frequency domain; and the computational complexity goal is also achieved. More specifically, the security in cryptosystems based on chaos can be increased using the derivative orders as secret keys in addition to the systems parameters [19], [20]; so the complexity of the verification of each key is strengthened causing the traditional cracking algorithms of chaotic masking will be unusable. Therefore, new fractional chaotic systems are crucial to enhance the performance of several integer-order chaos-based applications.

In this work, a fractional order unstable dissipative system (FOUDS) is analyzed, considering the dynamical characteristics of the integer-order UDS that have been previously reported [21]. we are interested in find a minimum effective order while chaos behavior is preserved in the first case. The fractional chaotic attractor appears as a result of the combination of several unstable one-spiral trajectories around a saddle hyperbolic stationary point. As second case, we also studied the trade-off between the equilibrium points and the reduction of effective dimension, which is the sum of all orders concerned to derivatives, in the proposed fractional order chaotic system. The resulting fractional chaotic attractor has same equilibria than scroll as shown herein. The fractional chaos state is verified using the time series analysis of the numerical temporal data.

Additionally, we also demonstrated the fractional chaotic attractor obtaining the topological horseshoe in both cases because not only provides much information that Lyapunov exponents, but also shows detailed dynamics of chaos, that is to say, a fractional order system should be chaotic if a horseshoe can be found to exist in it [22]. The reason to find a horseshoe must be Lyapunov exponents which seems insufficient to show chaotic characteristics of the fractional order systems, cause the numerical error may make it unreliable, especially when the computed output is close to zero.

2 Basic Definitions in Fractional Calculus

There are different definitions for fractional derivatives [2]. The Riemann-Liouville and the Caputo definitions are more reported than others [3]. The Caputo definition of the fractional derivative is,

$${}_0D_t^\alpha f(t) = \frac{1}{\Gamma(m-\alpha)} \int_0^t \frac{f^{(m)}(\tau)}{(t-\tau)^{\alpha+1-m}} d\tau, \quad (1)$$

where $m = \lceil \alpha \rceil$. The Riemann-Liouville definition can be described as

$${}_aD_t^\alpha f(t) = \frac{1}{\Gamma(n-\alpha)} \frac{d^n}{dt^n} \int_a^t (t-\tau)^{n-\alpha-1} f(\tau) d\tau, \quad (2)$$

where $n = \lceil \alpha \rceil$, and Γ is the Gamma function,

$$\Gamma(z) = \int_0^\infty t^{z-1} e^{-t} dt. \quad (3)$$

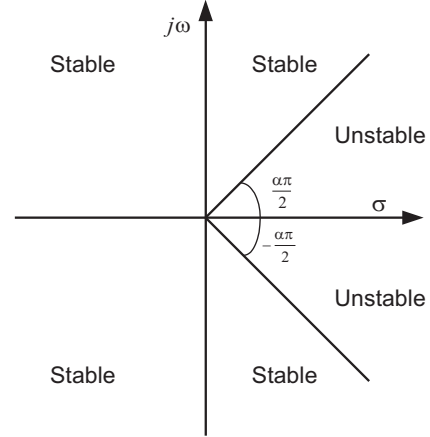


Fig. 1 Stability region of fractional order linear time invariant system with order $0 < \alpha < 1$

2.1 Numerical Method for Solving Fractional Differential Equations

We considered the Adams-Bashforth-Moulton method (ABM) [24], first we consider the following fractional differential equation:

$$\begin{aligned} D^\alpha(y(x) - y(0)) &= f(x, y(x)), \quad x > 0 \\ y^{(k)}(0) &= y_0^{(k)}, \quad k = 0, 1, \dots, m-1. \end{aligned} \quad (4)$$

The solution of (4) is given by a integral equation Volterra type as

$$y(x) = \sum_{k=0}^{\lceil \alpha \rceil - 1} y_0^{(k)} \frac{t^k}{k!} + \frac{1}{\Gamma(\alpha)} \int_0^x (x-z)^{\alpha-1} f(z, y(z)) dz. \quad (5)$$

How it is showed in [3], there is unique solution of (4) in $[0, X]$ interval, then we need to remplace (5) in a discrete form so

$$\begin{aligned} y_h(t_{n+1}) &= \sum_{k=0}^{\lceil \alpha \rceil - 1} y_0^{(k)} \frac{t^k}{k!} + \frac{h^\alpha}{\Gamma(\alpha+2)} f(t_{n+1}, y_h^P(t_{n+1})) \\ &+ \frac{h^\alpha}{\Gamma(\alpha+2)} \sum_{j=0}^{n+1} a_{j,n+1} f(t_j, y_h(t_j)), \end{aligned} \quad (6)$$

where

$$a_{j,n+1} = \begin{cases} n^{\alpha+1} - (n-\alpha)(n+1)^\alpha, & j=0, \\ (n-j+2)^{\alpha+1} + (n-j)^{\alpha+1} \\ -2(n-j+1)^{\alpha+1}, & 1 \leq j \leq n, \\ 1, & j=n+1, \end{cases} \quad (7)$$

The predictor has following structure

$$y_{n+1}^P = y(0) + \frac{1}{\Gamma(\alpha)} \sum_{j=0}^k b_{j,n+1} f(t_j, y_h(t_j)), \quad (8)$$

and $b_{j,k+1}$ is define by

$$b_{j,n+1} = \frac{h^\alpha}{\alpha} ((n+1-j)^\alpha - (k-j)^\alpha). \quad (9)$$

The error of this approximation is described as

$$\max_{j=0,1,\dots,N} |y(t_j) - y_h(t_j)| = O(h^p), \quad (10)$$

where $p = \min(2, 1 + \alpha)$.

2.2 Asymptotic Stability of the Fractional-Order System

Consider the following fractional-order dynamical system:

$$\frac{d^\alpha x}{dt} = Ax + Bu, \quad (11)$$

where $x \in R^n$, $u \in R^m$, and $A \in R^{n \times n}$, $B \in R^{n \times m}$, $p \equiv (x_1^*, x_2^*, x_3^*)$ be an equilibrium point of (11), and α is the fractional commensurate order.

Consider the following autonomous system

$$\frac{d^\alpha x}{dt} = Ax, \quad x(0) = x_0, \quad (12)$$

where A is $n \times n$ matrix, and $0 < \alpha < 1$ is asymptotically stable if and only if $|\arg \lambda| > \frac{\alpha\pi}{2}$ for all eigenvalues (λ) of A . In this case, each component of solution $x(t)$ decays towards 0 like $t^{-\alpha}$ [11]. This show that if $|\arg(\lambda)| > \frac{\alpha\pi}{2}$ for all eigenvalues (λ) of A then the solution $x_i(t)$ tends to 0 as $t \rightarrow \infty$. Thus, the equilibrium point p of the system is asymptotically stable if $|\arg(\lambda)| > \frac{\alpha\pi}{2}$, for all eigenvalues λ of A , that is if

$$\min_i |\arg(\lambda_i)| > \frac{\alpha\pi}{2} \quad (13)$$

The stable and unstable regions for $0 < \alpha < 1$ is shown in Fig. 1

Table 1 Equilibrium points and corresponding eigenvalues

Equilibrium point	Eigenvalues
$O(0, 0, 0)$	$-1.2041, 0.1020 \pm 1.1115i$
$E_1(0.66, 0, 0)$	$-1.2041, 0.1020 \pm 1.1115i$

3 Fractional Order Unstable Dissipative System - FOU DS

3.1 Unstable Dissipative System

The dynamical system is called unstable dissipative system (UDS) because it is dissipative in one of its components while unstable in the other two. The UDS is builded with a switching law to obtain a strange attractor. The strange attractor appear as a result of the combination of several unstable one-spiral trajectories. Each of these trajectories lies around a saddle hyperbolic stationary point. In [21] proposed a multiscroll attractor by switching linear systems

$$\begin{aligned} \dot{x} &= y, \\ \dot{y} &= z, \\ \dot{z} &= -ax - by - cz + f(x), \end{aligned} \quad (14)$$

where $a = 1.5$, $b = 1$, $c = 1$ and $\beta = 1$.

$$f(x) = \begin{cases} \beta, & \text{if } x \geq 0.35, \\ 0, & \text{otherwise} \end{cases} \quad (15)$$

The system (14) is dissipative if the sum of its eigenvalues is negative, additionally the system has three eigenvalues; one eigenvalue is a negative real number and two eigenvalues are complex numbers with positive real part.

3.2 Chaos generation in FOU DS

In this section, the corresponding fractional order system of (14), considering (15) as the switched function, is introduced and analyzed. The main idea consist on finding the minimum fractional order where the system exhibits chaos behavior using the same value for the system parameters as integer-order case. The resulting FOU DS is given by

$$\begin{aligned} D^\alpha x &= y, \\ D^\alpha y &= z, \\ D^\alpha z &= -ax - by - cz + f(x), \end{aligned} \quad (16)$$

where $\alpha \in (0, 1)$. The equilibrium points of the system (14) and the eigenvalues are given in Table 1, The system has only two equilibrium points, it is clear that them 0 and E_1 are saddle points of index two; hence, there are two-scroll attractor in the system (16).

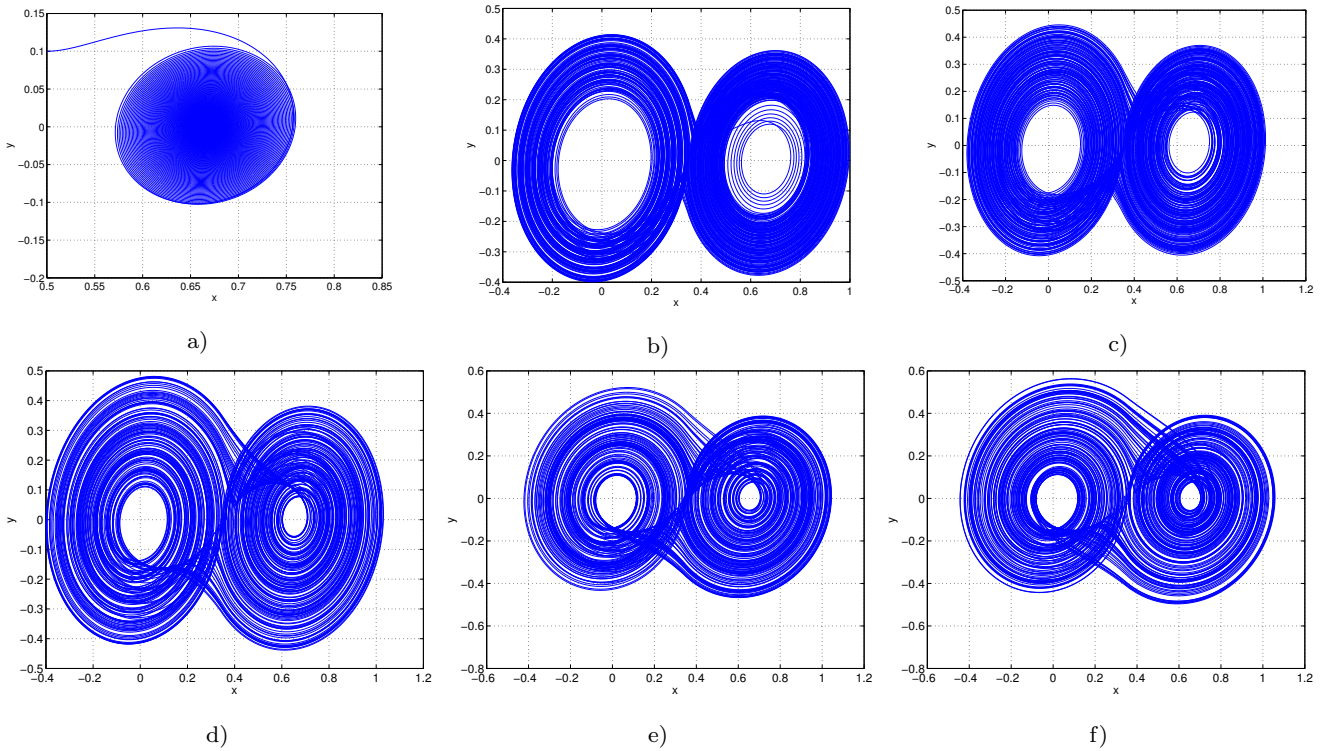


Fig. 2 xy -phase portraits for parameters given in Table 2

Table 2 Parameters which system in (16) generates chaotic behavior

Order α	System parameters	Behavior	LLE	Phase portrait
0.94	$a = 1.5, b = 1, c = 1, \beta = 1$	Fixed point		Fig. 2 a)
0.95	$a = 1.5, b = 1, c = 1, \beta = 1$	Chaos	0.44	Fig. 2 b)
0.96	$a = 1.5, b = 1, c = 1, \beta = 1$	Chaos	0.51	Fig. 2 c)
0.97	$a = 1.5, b = 1, c = 1, \beta = 1$	Chaos	0.51	Fig. 2 d)
0.98	$a = 1.5, b = 1, c = 1, \beta = 1$	Chaos	0.56	Fig. 2 e)
0.99	$a = 1.5, b = 1, c = 1, \beta = 1$	Chaos	0.6	Fig. 2 f)

In order to obtain fractional chaos from FOUDS, the stability general theorem given in (13) must be satisfied. As a result, the system (16) displays regular and stable behavior if

$$\alpha < \frac{2}{\pi} \min_i |\arg(\lambda_i)| \approx 0.9417 \quad (17)$$

Accordingly, the system does not show chaotic behavior for $\alpha < 0.9417$ as demonstrated in Fig 2 a) where the xy -phase portrait for $\alpha = 0.94$ is displayed.

It is found that FOUDS shows chaotic behavior for $\alpha \geq 0.95$. For $\alpha = 0.95$ xy -phase portrait is shown in Fig 2 b). Fig 2 c) to f) show xy -phase portraits to $\alpha = 0.96$ to $\alpha = 0.99$, respectively. This variety of fractional chaotic attractors have same equilibria than scrolls.

The largest Lyapunov exponents (LE) λ_{\max} of the fractional chaotic attractors in Fig 2 are computed from the numerical time series of the state-variable x . As well-known, a positive LE indicates chaos behavior. The

higher the value of the LE, the higher the chaoticity observed in a system.

Table 2 shows the numerical results of largest LE using TISEAN package software [25]. TISEAN has been appointed as a proved tool to investigate the presence of chaos in several numerical and experimental systems.

3.3 Chaos in Lowest Orders of FOUDS

As mentioned in introduction, one viable application of the fractional chaotic systems consist on using the fractional derivative order as the key for secure communications schemes. So the lower the value of the fractional order, the higher the number of possible combinations for the secret key. Thus, the FOUDS is modified to obtain a lower order than previous case. By considering the strange attractor appears as a result of the combination of several unstable one-spiral trajectories around

Table 3 Parameters which system in (16) generates regular oscillations and chaotic behavior

	Order α	System parameters	Behavior	LLE	Phase portrait
i)	0.7	$a = 7.5, b = 0.2, c = 0.2, \beta = 5$	Limit cycle		Fig. 3 a)
ii)	0.74	$a = 4.5, b = 0.3, c = 0.3, \beta = 3$	Limit cycle		Fig. 3 b)
iii)	0.77	$a = 3, b = 0.5, c = 0.5, \beta = 3$	Limit cycle		Fig. 3 c)
iv)	0.8	$a = 3.75, b = 0.7, c = 0.7, \beta = 2.5$	Chaos	0.4	Fig. 3 d)
v)	0.82	$a = 4.75, b = 0.9, c = 0.9, \beta = 3.16$	Chaos	0.53	Fig. 3 e)
	0.83	$a = 4.75, b = 0.9, c = 0.9, \beta = 3.16$	Chaos	0.66	Fig. 3 f)

a saddle hyperbolic stationary point, the equilibrium points together with the commutation plane are scaled in a proper form to preserve the chaos regimen and the asymptotically stability.

This is carried out by choosing other set of the system parameters a, b, c and function $f(x)$ to satisfy the stability condition in (13). Analogous to previous case, FOUDS in (16) generates both regular oscillations and chaotic behaviors. Numerical results, lower order, system parameters and the corresponding largest LE are given in Table 3 and Fig 3.

4 Topological Horseshoe Theory

The topological horseshoe theory, which is based on the notion of symbolic dynamics[22]-[30], provides a rigorous proof to estimate topological entropy, verify existence of chaos, and reveal invariant sets of chaotic attractors in chaotic systems. The topological horseshoe depends on the geometry of continuous maps on some subsets of interest in state space based on the second return Poincaré map, for continuous-time systems the topological horseshoe theorem cannot be directly applied [23]. Therefore, one needs to find an appropriate Poincaré section to obtain an appropriate Poincaré map.

In this work, the topological horseshoe of FOUDS is determined in both aforementioned cases because not only provides much information that Lyapunov exponents, but also shows detailed dynamics of chaos, that is to say, a fractional order system should be chaotic if a horseshoe can be found to exist in it [22].

The basic procedure is to propose an appropriate Poincaré section and define a second return Poincaré map, which implies that the entropy of the attractors of FOUDS is not less than $\log 2$, proving the existence of chaos. The reason to find a horseshoe must be Lyapunov exponents which seems insufficient to show chaotic characteristics of the fractional order systems,

cause the numerical error may make it unreliable, especially when the computed output is close to zero.

4.1 Aspects of symbolic dynamics

Let $S_m = \{0, 1, \dots, m-1\}$ and \sum_m be the collection of all bi-infinite sequences with their elements $s \in \sum_m$:

$$s = \{\dots, s_{-n}, \dots, s_{-1}, s_0, s_1, \dots, s_n, \dots\}, \quad s_i \in S_m, \forall i.$$

If we consider another sequence $\bar{s} \in \sum_m$, with

$$\bar{s} = \{\dots, \bar{s}_{-n}, \dots, \bar{s}_{-1}, \bar{s}_0, \bar{s}_1, \dots, \bar{s}_n, \dots\}, \quad \bar{s}_i \in S_m, \forall i.$$

Then the distance between s and \bar{s} is defined as

$$d(s, \bar{s}) = \sum_{-\infty}^{\infty} \frac{1}{2^{|i|}} \frac{|s_i - \bar{s}_i|}{1 + |s_i - \bar{s}_i|}. \quad (18)$$

4.2 Metric space and the m -shift

With the distance defined in (18), \sum_m is a metric space and has the following three properties with which a set is called a Cantor set.

Theorem 1 [28] *The metric space \sum_m is*

- (i) *compact;*
- (ii) *totally disconnected;*
- (iii) *perfect.*

Now define a map of \sum_m into itself, denoted by γ , as follows:

$$\gamma(s)_i = s_{i+1} \quad \forall i \quad (19)$$

The map γ is referred to as the m -shift map, which has the following properties.

Theorem 2 [22] (a) $\gamma(\sum_m) = \sum_m$, and γ is continuous; (b) *The shift map γ as a dynamical system defined*

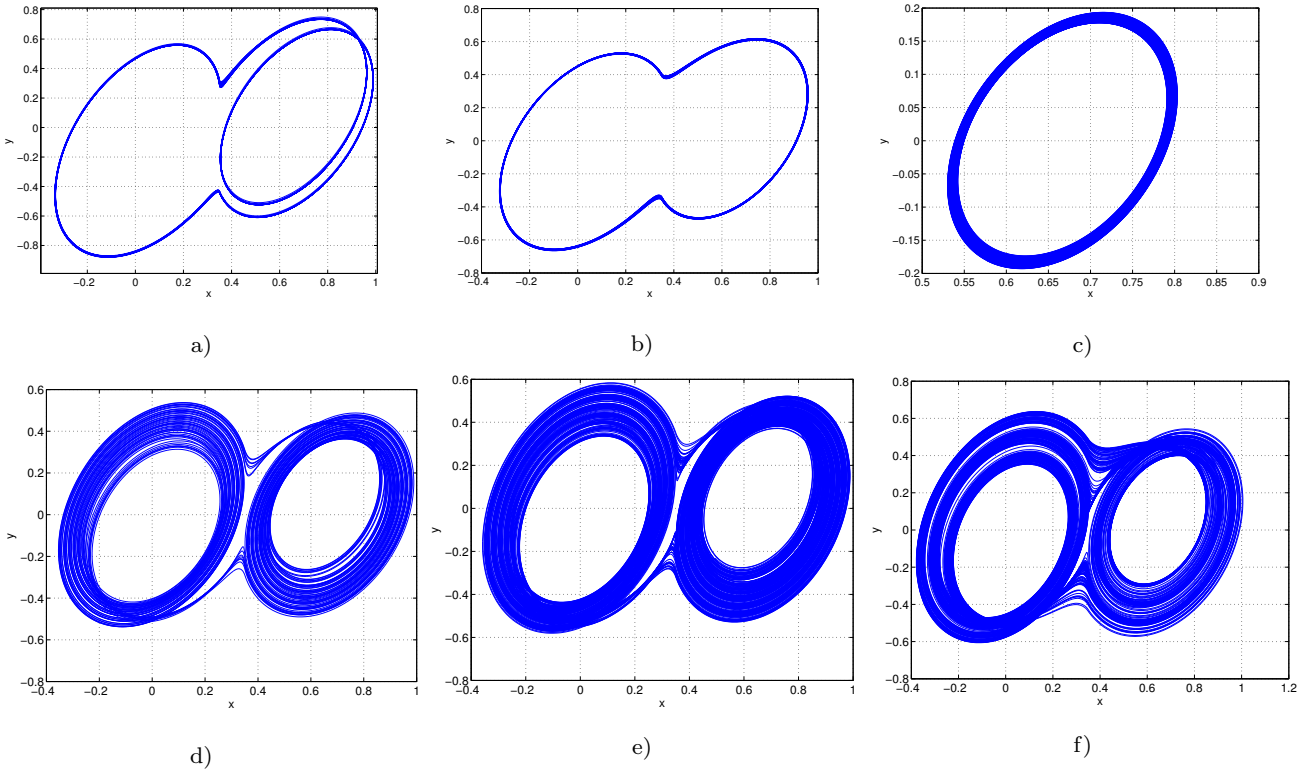


Fig. 3 xy -phase portraits for parameters given in Table 3

on \sum_m has:

- (i) a countable infinity of periodic orbits consisting of orbits of all periods;
- (ii) an un-countable infinity of non-periodic orbits;
- (iii) a dense orbit.

In this manner the dynamics generated by the shift map γ display sensitive dependence on initial conditions on a closed invariant set, and therefore are chaotic. (See [22]-[30] for proofs of the theorems.)

Let X be a metric space, D be a compact subset of X , and $f : D \rightarrow X$ be a map satisfying the assumption that there exist m mutually disjoint subsets D_1, \dots, D_{m-1} and D_m of D , so that the restriction of f to each D_i , $f|_{D_i}$, is continuous, for all $i = 1, \dots, m-1$.

Definition 1 [27]-[28] Let ξ be a compact subset of D , such that for every $1 \leq i \leq m$, $\xi_i = \xi \cap D_i$ is nonempty and compact. Then ξ is called a connection with respect to D_1, \dots, D_{m-1} and D_m . Let F be a family of connections with respect to D_1, \dots, D_{m-1} and D_m , satisfying the property:

$$\xi \in F \Rightarrow f(\xi_i) \in F.$$

Then F said to be a f -connected family with respect to D_1, \dots, D_{m-1} and D_m .

Definition 2 [22] If there is a continuous and onto map

$$h : K \rightarrow \sum_m$$

such that $h \circ f = \gamma \circ h$, then f is said to be a semi-conjugate to γ .

Theorem 3 [22]-[27] If there is an f -connection family with respect to D_1, D_2, \dots, D_m , then there is a compact invariant set $K \subset D$, such that $f|_K$ is semi-conjugate to an m -shift map.

Theorem 4 [29] For two dynamical systems (X, f) and (Y, g) , if (X, f) is semi-conjugate to (Y, g) , then the topological entropy of f is not less than g .

The topological entropy is a nonnegative real number. Then the system is chaotic if its topological entropy is not zero. Furthermore, if g is an m -shift map, then $ent(f) \geq ent(g) = \log m$, that is, f is chaotic when $m > 1$.

4.3 Topological Horseshoe in the proposed FOUDS

In this subsection, we prove the existence of the horseshoe in the fractional-order system (16) based on the review in the section above.

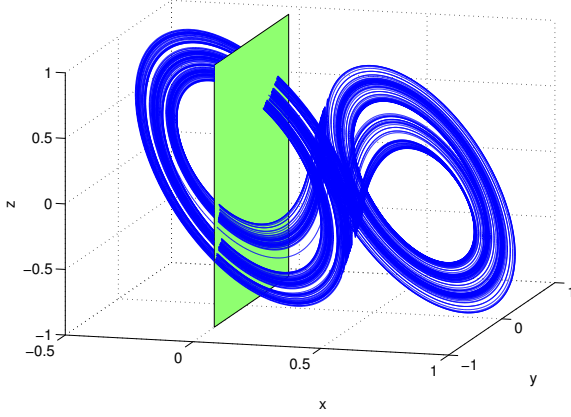


Fig. 4 xy -phase portrait for parameters given in Table 3

Considering the fractional-order system (16) with $a = 4.75, b = 0.9, c = 0.9, \beta = 3.16$, first consider the plane $\Omega = \{(x, y, z) \in R^3 : x = 0\}$ as shown in Fig 4. On this plane, choose a Poincaré section with its four vertices being

$$A(0, 0.35, 0.44), B(0, 0.44, 0.46),$$

$$C(0, 0.46, 0.45), D(0, 0.34, 0.41)$$

The Poincaré map

$$P : |ABCD| \rightarrow \Omega,$$

is defined as follows. For each point $x \in |ABCD|$, $P(x)$ is chosen to be the first return intersection point with Ω under the flow of the system (16) with initials condition x . Under this Poincaré map P , $P(x)$ is very thin hook-like strip which is wholly across $|ABCD|$ as shown in Fig 5, where

$$A' = P(A), B' = P(B), C' = P(C), D' = P(D),$$

are the images of points, respectively.

Theorem 5 *The Poincaré map P corresponding to the Poincaré section $|ABCD|$ has the property that there is a closed invariant set $\Lambda \subset |ABCD|$ for which $P|_{\Lambda}$ is semi conjugate to the 2-shift map, Hence, $(P) \geq \log 2 > 0$. This implies that attractor generated by system (16) with $a = 4.75, b = 0.9, c = 0.9, \beta = 3.16$, has a positive topological entropy.*

Proof. In order to prove the assertion, one must find two mutually disjoint subsets of $|ABCD|$, such that a P -connected family with respect to them exists.

The subsets are denoted by Q_1 and Q_2 as shown in Fig 5, the first subset Q_1 with the quadrangle $|AEFD|$. Under the first return Poincaré map P , the subset Q_1 is mapped to $|A'D'E'F'|$ with AD mapped to $A'D'$ and EF mapped to $E'F'$. We can make the conclusion that the image $P(Q_1)$ lies wholly across the quadrangle $|ABCD|$ with respect to AD and BC as shown in the Fig 6.

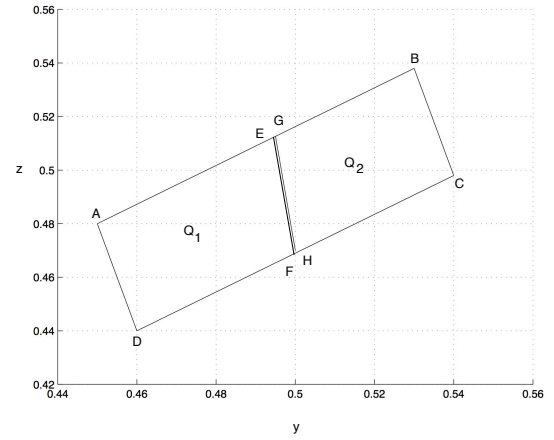


Fig. 5 Two mutually disjoint subsets $|AEFD|$ and $|GBCH|$ of the quadrangle $|ABCD|$

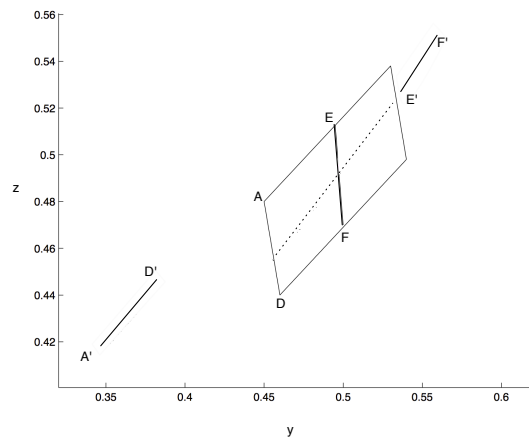


Fig. 6 The image $|A'E'F'D'|$ of the quadrangle $|AEFD|$ under the map P .

The second subset Q_2 , namely quadrangle $|GBCH|$, with GH and BC being its bottom and top edges,

respectively. Like Q_1 the subset Q_2 is mapped to $|G'B'C'H'|$ under the Poincaré map P with GH mapped to $G'H'$ and BC mapped to $B'C'$. Thus, the image $P(Q_2)$ lies wholly across the quadrangle $|ABCD|$ with respect to AD and BC as shown in the Fig 7.

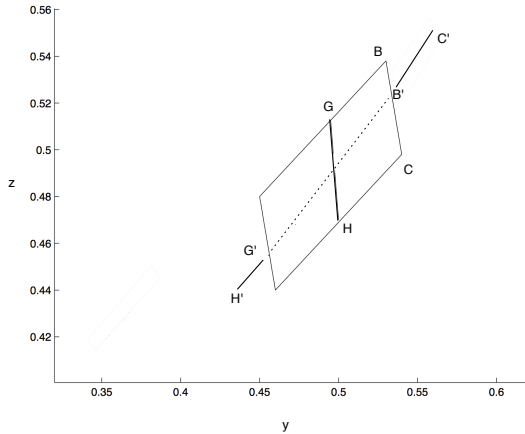


Fig. 7 The image $|G'B'C'H'|$ of the quadrangle $|GBCH|$ under the map P .

Evidently, the subsets Q_1 and Q_2 are mutually disjoint. Therefore, it follows that for every connection of $|ABCD|$ respect Q_1 and Q_2 , for instance, Q_5 , the images $P(Q_5 \cap Q_1)$ and $P(Q_5 \cap Q_2)$ also lie wholly across the quadrangle $|ABCD|$. Thus the images of $P(Q_5 \cap Q_1)$ and $P(Q_5 \cap Q_2)$ are still connections respect to Q_1 and Q_2 . According to Definition 1 and Theorem 3, there is a P -connected family, so that the Poincaré map P is semi conjugate to the 2-shift map. Based on Theorem 4, it is concluded that the entropy of P is not less than $\log 2$, which implies that the attractor has positive entropy. The proof is completed

All this facts prove that the fractional order unstable dissipative system attractor has positive topological entropy, and hence it is chaotic.

Similar to previous case, now we applied the same proof to demonstrate a topological horseshoe when selected $a = 4.75, b = 0.7, c = 0.7, \beta = 2.5$, parameters and consider an order $\alpha = 0.8$, the attractor corresponding is showed at Fig 3 d) in this plane, choose a Poincaré section with its four vertices being

$$\hat{A}(0, 0.4, 0.45), \hat{B}(0, 0.45, 0.475),$$

$$\hat{C}(0, 0.45, 0.4), \hat{D}(0, 0.5, 0.45)$$

The Poincaré map

$$\hat{P} : |\hat{A}\hat{B}\hat{C}\hat{D}| \rightarrow \hat{\Omega},$$

is defined as follows. For each point $x \in |\hat{A}\hat{B}\hat{C}\hat{D}|$, $\hat{P}(x)$ is chosen to be the first return intersection point with $\hat{\Omega}$ under the flow of the system (16) with initials condition x . Under this Poincaré map \hat{P} , $\hat{P}(x)$ is very thin hook-like strip which is wholly across $|\hat{A}\hat{B}\hat{C}\hat{D}|$ as shown in Fig 8, where

$$\hat{A}' = \hat{P}(\hat{A}), \hat{B}' = \hat{P}(\hat{B}), \hat{C}' = \hat{P}(\hat{C}), \hat{D}' = \hat{P}(\hat{D}),$$

are the images of points, respectively.

Theorem 6 *The Poincaré map P corresponding to the Poincaré section $|\hat{A}\hat{B}\hat{C}\hat{D}|$ has the property that there is a closed invariant set $\hat{A} \subset |\hat{A}\hat{B}\hat{C}\hat{D}|$ for which $\hat{P}|_{\hat{A}}$ is semi conjugate to the 2-shift map, Hence, $(\hat{P}) \geq \log 2 > 0$. This implies that attractor generated by system (16) with $a = 4.75, b = 0.7, c = 0.7, \beta = 2.5$, has a positive topological entropy.*

Proof. In order to prove the assertion, one must find two mutually disjoint subsets of $|\hat{A}\hat{B}\hat{C}\hat{D}|$, such that a \hat{P} -connected family with respect to them exists.

The subsets are denoted by Q_3 and Q_4 as shown in Fig 8, the first subset Q_3 with the quadrangle $|\hat{A}\hat{D}\hat{E}\hat{F}|$. Under the first return Poincaré map \hat{P} , the subset Q_3 is mapped to $|\hat{A}'\hat{D}'\hat{E}'\hat{F}'|$ with $\hat{A}\hat{D}$ mapped to $\hat{A}'\hat{D}'$ and $\hat{E}\hat{F}$ mapped to $\hat{E}'\hat{F}'$. We can make the conclusion that the image $\hat{P}(Q_3)$ lies wholly across the quadrangle $|\hat{A}\hat{B}\hat{C}\hat{D}|$ with respect to $\hat{A}\hat{D}$ and $\hat{B}\hat{C}$ as shown in the Fig 8.

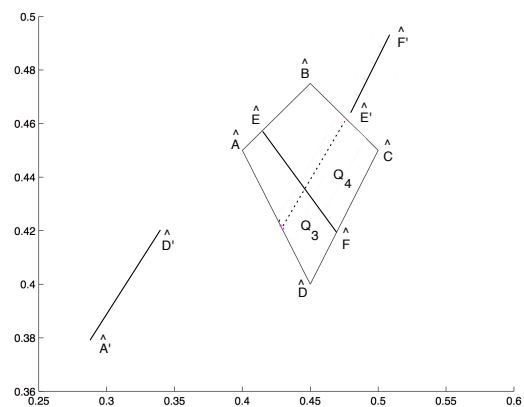


Fig. 8 The image $|\hat{A}'\hat{E}'\hat{F}'\hat{D}'|$ of the quadrangle $|\hat{A}\hat{E}\hat{F}\hat{D}|$ under the map \hat{P} .

The second subset Q_4 , namely quadrangle $|\hat{G}\hat{B}\hat{C}\hat{H}|$, with $\hat{G}\hat{H}$ and $\hat{B}\hat{C}$ being its bottom and top edges, respectively. Like Q_3 the subset Q_4 is mapped to $|\hat{G}'\hat{B}'\hat{C}'\hat{H}'|$ under the Poincaré map \hat{P} with $\hat{G}\hat{H}$ mapped to $\hat{G}'\hat{H}'$ and $\hat{B}\hat{C}$ mapped to $\hat{B}'\hat{C}'$. Thus, the image $P(Q_4)$ lies wholly across the quadrangle $|\hat{A}\hat{B}\hat{C}\hat{D}|$ with respect to $\hat{A}\hat{D}$ and $\hat{B}\hat{C}$ as shown in the Fig 8.

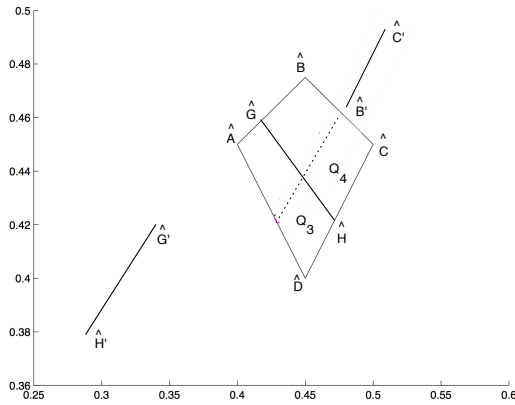


Fig. 9 The image $|\hat{G}'\hat{B}'\hat{C}'\hat{H}'|$ of the quadrangle $|\hat{G}\hat{B}\hat{C}\hat{H}|$ under the map \hat{P} .

Evidently, the subsets Q_3 and Q_4 are mutually disjoint. Therefore, it follows that for every connection of $|\hat{A}\hat{B}\hat{C}\hat{D}|$ respect Q_3 and Q_4 , for instance, Q_6 , the images $P(Q_6 \cap Q_3)$ and $P(Q_6 \cap Q_4)$ also lie wholly across the quadrangle $|\hat{A}\hat{B}\hat{C}\hat{D}|$. Thus the images of $P(Q_6 \cap Q_3)$ and $P(Q_6 \cap Q_4)$ are still connections respect to Q_3 and Q_4 . According to Definition 1 and Theorem 3, there is a P -connected family, so that the Poincaré map \hat{P} is semi conjugate to the 2-shift map. Based on Theorem 4, it is concluded that the entropy of \hat{P} is not less than $\log 2$, which implies that the attractor has positive entropy. The proof is completed

All this facts prove that the fractional order unstable dissipative system attractor has positive topological entropy, and hence it is chaotic.

5 Conclusion

We have studied a fractional order system and analyzed its chaotic characteristic by applying the topological horseshoe theory a proof has been given to confirm that the entropy of P is not less than $\log 2$ in fractional order unstable dissipative system, further we considered the largest Lyapunov exponent to prove the chaotic behavior its system.

Acknowledgements CONACYT

References

1. Grzesikiewicz, W., Wakulicz, Andrzej., Zbiciak, A.: Non-linear problems of fractional calculus in modeling of mechanical systems. *International Journal of Mechanical Sci* 70. 90-98 (2013)
2. Podlubny, I.: *Fractional Differential Equations*. Academic Press, New York (1999)
3. Diethelm, K.: *The Analysis of Fractional Differential Equations, An Application-Oriented Exposition Using Differential Operators of Caputo Type*. Springer-Verlag, Berlin (2010)
4. Rakkiyappan, R., Velmurugan G., Cao, J.: Stability analysis of memristor-based fractional-order neuronal networks with different memductance function. *Cogn Neurodyn* 9. 145-177 (2015)
5. Ghasemi, S., Tabesh, A., Askari-Marnani, J.: Application of fractional calculus theory to robust controller design for wind turbine generators. *IEEE Trans. On Energy Conversion* 29. 780-787 (2014)
6. Bhalekar, S.: Synchronization of incommensurate non-identical fractional order chaotic systems using active control. *Eur. Phys. J. Special Topics* 223, 1495-1508 (2014)
7. Sasso, A., Palmieri, G., Amodio, D.: Application of fractional derivative models in linear viscoelastic problems. *Mech Time-Depend Mater* 15. 367-387 (2011)
8. Guyomar, D., Ducharne, B., Sebald, G., Audiger, D.: Fractional Derivative Operators for Modeling the Dynamic Polarization Behavior as a Function of Frequency and Electric Field Amplitude. *IEEE Transactions on Ultrasonics, Ferroelectric, and Frequency Control* 56. 437-443 (2009)
9. Monje, C. A., Chen, YQ., Vinagre, B. M., Xue, D., Feliu, V.: *Fractional-order Systems and Controls, Fundamentals and Applications*. Springer-Verlag, London (2010)
10. Zhang, R., Yang, Shipping.: Adaptive synchronization of fractional-order chaotic systems via a single driving variable. *Nonlinear Dynamics* 66. 831-837 (2011)
11. Petras. I.: *Fractional-Order Nonlinear Systems, Modeling, Analysis And Simulation*. Higher Education Press, Beijing and Springer-Verlag, Berlin Heidelberg (2011)
12. Grigorenko, I., Grigorenko, E.: Chaotic dynamics of the fractional Lorenz system. *Phys. Rev. Lett.* 91, 034101 (2003)
13. Lu, J.G., Chen, G.: A note on the fractional order Chen system. *Chaos Solitons Fractals* 27(3), 685-688 (2006)
14. Hartley, T.T., Lorenzo, C.F., Qammer, H.K.: Chaos in a fractional order Chua's system. *IEEE Trans. Circuits Syst. I* 42, 485-490 (1995)
15. Li, C., Chen, G.: Chaos and hyperchaos in the fractional-order Rössler equations. *Physica A* 341. 55-61 (2004)
16. Ahmad, W.M., Sprott, J.C.: Chaos in fractional order autonomous nonlinear systems. *Chaos Solitons Fractals* 16, 339-351 (2003)
17. Lu, J.G., Chen, G.: A note on the fractional order Chen system. *Chaos Solitons Fractals* 27(3), 685-688 (2006)
18. HosseinNia, S. H., Magin, R. L., Vinagre, B. M.: Chaos in fractional and integer order NSG systems. *Signal Processing* 107. 302-311 (2015)
19. Ma, T., Zhang, J.: Hybrid synchronization of coupled fractional-order complex networks. *Neurocomputing* 157. 166-172 (2015)

20. Kiani-B, A., Fallahi, k., Pariz, N., Leung, Henry.: A chaotic secure communication scheme using fractional chaotic systems based on an extended fractional Kalman filter. *Communications in Nonlinear Science and Numerical Simulation* 14, 863-879 (2009)
21. Campos-Canton, E., Barajas-Ramirez, J. G., Solis-Perales, G., Femat, R.: Multiscroll attractors by switching systems, *American Institute of Physics. Chaos* 20, 013116/6 (2010)
22. Wiggins, S.: *Introduction to Applied Nonlinear Dynamical Systems and Chaos*. Springer, New York (1990)
23. Yang, X.S., Yu, Y.G., Zhang, S.C.: A new proof for existence of horseshoe in the Rössler system. *Chaos Solitons Fractals* 18, 223-227 (2003)
24. Diethelm, K., Neville, F., Freed. A. D.: A Predictor-Corrector Approach for the Numerical Solution of Fractional Differential Equations. *Nonlinear Dynamics* 29, 3-22 (2002)
25. Hegger, R., Kantz, H., Schreiber, T.: Practical implementation of nonlinear time series methods: The TISEAN package, *CHAOS* 9, 413 (1999)
26. Yang, X.S., Tang, Y.: Horseshoes in piecewise continuous maps. *Chaos Solitons Fractals* 19, 841-845 (2004)
27. Jia, H. Y., Chen, Z. Q., Qi, G. Y.: Chaotic Characteristics analysis and circuit implementation for a fractional-order system. *IEEE Trans. Circuits Syst. I* 61, 845-853 (2014)
28. Yang, X.S., Yu, Y.G., Zhang, S.C.: A new proof for existence of horseshoe in the Rössler system. *Chaos Solitons Fractals* 18, 223-227 (2003)
29. Topological horseshoe analysis and circuit realization for a fractional-order Lü system. *Nonlinear Dyn* 74, 203-212 (2013)
30. Wu, W.J., Chen, Z.Q., Yuan, Z.Z.: A computer-assisted proof for the existence of horseshoe in a novel chaotic system. *Chaos Solitons Fractals* 41, 2756-2761 (2009)